ATLANTIS PRESS

Atlantis Highlights in Engineering (AHE), volume 1

International Conference on Science and Technology (ICST 2018)

Morphology and Porosity of Fe_3O_4@SiO_2 Core-Shell: Adsorption for Heavy Metal Pb(II)

M. Munasir[1], Novi Setyaningsih, Sari Yanasin, Z.A Imam Supardi

Physics Department

Universitas Negeri Surabaya

Surabaya, Indonesia

[1]munasir_physics@unesa.ac.id

***Abstract*—The Analysis of morphology, porosity and absorption of Fe_3O_4 nano particles coated with SiO_2-NPs has been carried out; use polyethelen glycol as a core for forming core-shell Fe_3O_4@ SiO_2/PEG. SiO_2-NPs is prepared from quartz sand by hydrothermal and coprecipitation methods; Fe_3O_4-NPs have been prepared from iron sand with the co-precipitation method. Characterization of morphology with SEM-EDX; porosity (Ap, Vp, Dp) using BET (adsorption and disorption); and Pb (II) adsorption with AAS. Obtained the larger particle size, the lower porous for the less SiO_2-NPs composition. The best formation of core-shell composition is Fe_3O_4@ SiO_2 /PEG for Fe_3O_4 and SiO_2 (composition 1:1; 1:3 and 3:1), the largest Pb (II) adsorption rate of 2.34 mg/g and absorbed concentration of Pb (II) 23.4 mg /l.**

Keywords: marphology; porosity; Core-shell; Fe_3O_4-NPs; Pb(II)

I. INTRODUCTION

Recently, the research of nanoparticles (NPs) Fe_3O_4 and SiO_2, and their composite formation, forming core-shell formations, are very much in demand, hundreds of researchers around the world are studying and searching for formulas and various modifications for various technology applications that are currently developing with fast. It is known that Fe_3O_4-NPs which have super paramagnetic properties, can be synthesized from abundant iron sand minerals in Indonesia, this material has broad application prospects, such as: biocompatible [1], biosensing [2], contras agent for MRI system [3], Drug Delivary System [4], absorbent heavy-metal (Cr, Pb, Ag) [5], [6]. The same thing for SiO_2-NPs has inert properties which are good insulators and are not easy to react with chemical compounds, high porosity, low thermal conductive; can be synthesized from quartz sand, and organic materials of rice-husk ash, baggase-ash which is abundantly available in Indonesia; SiO_2-NPs has a wide range of applications, such as: anti-aging material [7], divice-optoelectronic [8], coating anti-corrosion [9], DDS [10], cosmetic [11], water-filter system [12], adsoption for hevy-metal [10], [13], packaging system [11], etc.

The formation of Fe_3O_4@SiO_2 core-shell material is a development research for further complex applications such as contrast-agent systems on MRI-based medical systems [3], [14] or for drug transport system DDS, for the treatment of tissue damage caused by cancer [15], also applications in filtration systems, and desalination of clean water [8], [16]. In this research report, I will report the synthesis of new core-shell Fe_3O_4@SiO_2 /PEG, PEG as a binder, with a focus on the study of microstructure through SEM-EDS, porosity test with BET and BJH test, also adsorption test on heavy- metal Pb (II).

II. MATERIALS AND METHOD

A. Materials

The main ingredients prepared are raw material in the form of: iron sand and quartz sand that has been mashed and cleaned from other organic and natural organic impurities, chemicals such as alkaline compounds (NaOH, KOH or Na_2CO_3), hydrochloric acid (HCl) PA (37 %), and NH_4OH, pH-meter, and distilled water (DI-Water).

B. Synthesis and Characterization

Preparation of SiO_2 nanoparticles using the extraction and hydrothermal methods to obtain sodium silicate (Na_2O .$xSiO_{3(aq)}$) as a precursor, followed by the co-precipitation method, the addition of HCl (5M) to the precursor. The final stage of the silgel slurry whasing and drying process becomes silica powder ($Si(O)_{(aq)} \rightarrow SiO_{2(s)}$)[8]. And the preparation of Fe3O4 nanoparticles was carried out by means of magnetic sparation for the preparation of high purity iron oxide powder, then dissolved in HCl (12 Molar) as well as for the formation of precursors $FeCl_3$ and $FeCl_2$, then continued with the addition of NH_4OH solution (co-precipitation method), so obtained nano-size iron oxide deposits: Fe_3O_4 ($Fe_3O_{4(s)}$+ $8NH_4Cl_{(l)}+5H_2O_{(l)} \rightarrow Fe_3O_{4(s)}$)[7], [8]. Furthermore, Poly-ethylene glycol (PEG) was mixed with Fe_3O_4-NPs and distorted until homogeneous, then SiO2-NPs was added, with wet mixing method, so that Fe_3O_4 @ SiO2 / PEG was obtained, with a ratio of Fe_3O_4 and SiO_2 is 1: 1; 1: 3 and 3: 1. Microstructure and quantity of atoms / constituent elements were analyzed by SEM-EDS; analysis of porous surface area (Ap) porous volume (Vp) and porous diamter (Dp) using BET-BJH.

III. RESULT AND DISCUSSION

Characterization of Fe_3O_4/SiO_2 core-shell samples includes a microstructure profile, looking at the particle shape and particle size as well as formation information and homogeneity of the SiO_2 and Fe_3O_4 particles composition, core-shell system, also quantity analysis and distribution of constituent elements.

A. Phase and Structure Crystal

Crystal structure profiles of SiO_2 nanoparticles, Fe_3O_4 nanoparticles and in Fe_3O_4/SiO_2 core-shell formations; presented in Figure 1.

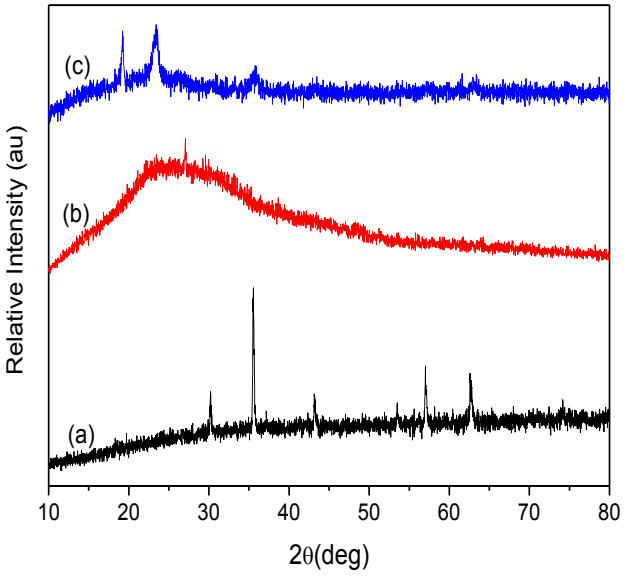

Fig. 1. Pattern of XR-Diffraction of (a) Fe_3O_4 NPs ; (b) SiO_2 and (c) core-shell $Fe_3O_4@SiO_2$

That SiO_2-NPs shows an amorphous phase, although there are already indications that the quarzt phase (2θ ~26°) is formed; whereas for Fe_3O_4-NPs it forms crystals with the magnetite phase; and Fe_3O_4/SiO_2 core-shell, magnetite crystal peaks are less visible, because covered by amorphous SiO2; in a different position a new peak is identified as PEG (2θ~18-24°).

B. Microstructure

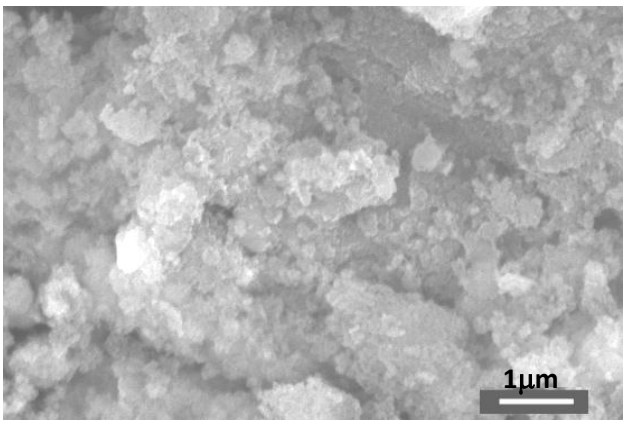

Fig. 2. Microstructure of Fe_3O_4/SiO_2-NCs (#sample-1)

In Figure 2, the core-shell $Fe_3O_4@SiO_2$ morphology (sample # 1), appears to have several voids, irregular particle formations. This happens because most of the SiO2 is speroid and Fe_3O_4 is not uniformly distributed. The average particle size of $Fe_3O_4@SiO_2$ was estimated to be ~ 74 nm with elements of O, Si and Fe at 64.14%, 28.94% and 6.91% respectively (shown in Fig. 3).

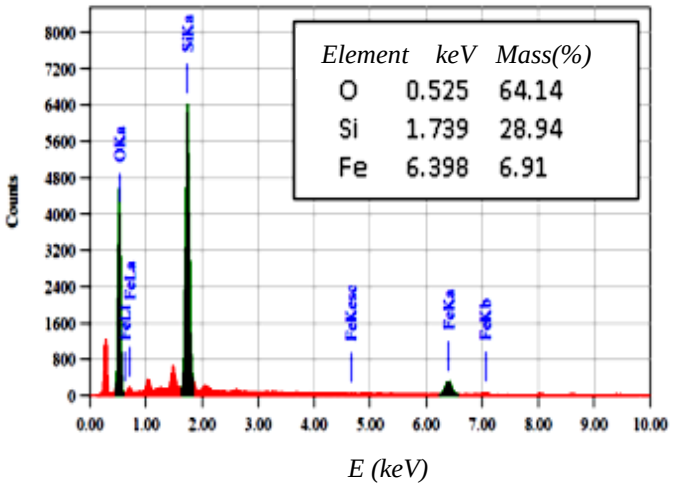

Fig. 3. EDS of Fe_3O_4/SiO_2-NCs (#sample-1)

In Figure 4, the morphology of ncore-shell $Fe_3O_4@SiO_2$ is shown for sample # 2 with a ratio of Fe_3O_4 and SiO2 1: 3. Microstructure profile is generally the same as sample # 1, SiO_2 oxide spread is more dominant, covering the presence of Fe_3O_4, this is in line with the composition of mixing where SiO_2 is more abundant. The average particle size of Fe_3O_4 @ SiO_2 core-shell was estimated at ~ 120 nm with elements of O, Si and Fe at 62.74%, 36.66% and 0.60% respectively (shown in Fig. 5).

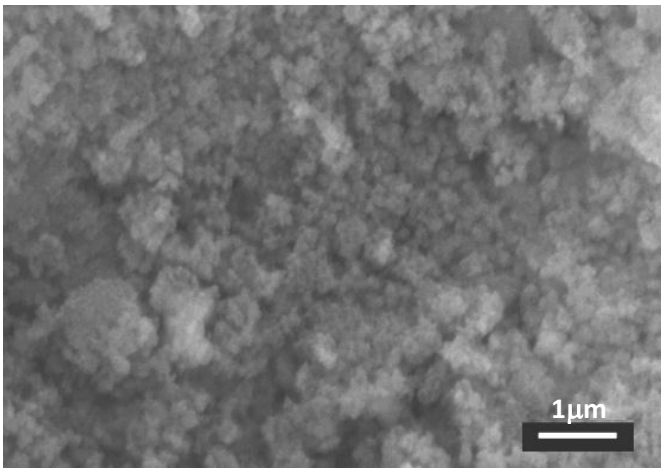

Fig. 4. Microstructure of Fe_3O_4/SiO_2-NCs (#sample-2)

In Figure 6, a micro profile of the core-shell $Fe_3O_4@$ SiO_2 sample (Sample # 3) appears, where the ratio of Fe_3O_4 and SiO2 is 3:1, the dominant is Fe3O4. Based on the opposite composition with sample #2, it appears that SiO_2 oxide is substituted in aglomersed Fe_3O_4; there are voids in core-shell particles, the core-shell particle size of $Fe_3O_4@SiO_2$ is estimated to be ~142.8 nm and the results of the analysis with EDS, it is obtained that the content of O, Si and Fe elements is 66.08%, 30.57% and 3.35% respectively-according to (shown in Fig. 7).

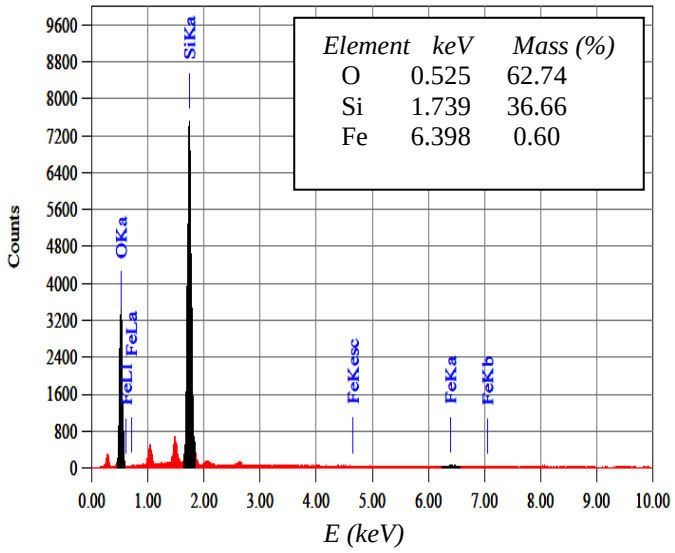

Fig. 5. EDS of Fe_3O_4/SiO_2-NCs (#sample-2)

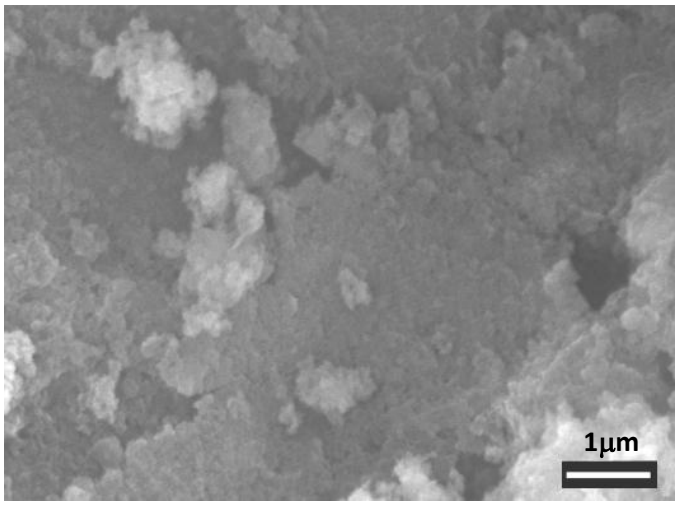

Fig. 6. Hasil uji SEM EDX sampel 3

Overall, the results of EDX analysis show that the elements of domina detected are O, Si, and Fe. And quantitatively the composition of the sample formation: 1: 1 (sample # 1), 1: 3 (sample # 3), and 3: 1 (sample # 3), is not consistent with the quantity of atomic elements of the feeder, due to mass comparison. It appears in sample # 1 that the elemental content of Fe is the highest, while in sample # 3, even though the mass composition composition of Fe3O4 is more (0.75gram) and SiO2 (0.25 grams), without the element of Fe Fe is less (3.35%) if compared to sample # 2. And in general the particle size of core-shell material is nanometer (~ 100 nm).

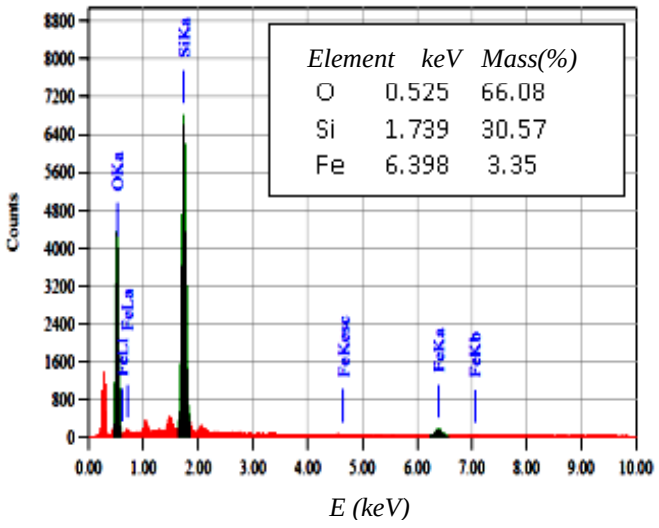

Fig. 7. EDS of Fe_3O_4/SiO_2-NCs (#sample-3)

C. BET and Porosity

BET (Brunaeur-Emmet-Teller) is a method to measure the porosity of a solid material, the data is an adsorption graph and is absorbed by N_2 (Nitrogen) gas which is passed to the pores of the material, so that information on porous surface area (Ap) is obtained, estimated by BET, porous diameter (Dp) and volume porous (Vp), which later in the BET test also obtained BJH-method data analysis and DH-method.

TABLE I. POROUS DIAMTER (DP) Fe_3O_4@SiO_2 *CORE SHELL*

Sample	Diameter Pori (Å)				
	BET	Metode BJH		Metode DH	
		Adp	Desp	Adp	Desp
#1	88,07	754	17,20	754	17,20
#2	912,8	15,43	16,91	15,43	16,91
#3	205,7	17,04	15,23	17,04	15,23

TABLE II. POROUS SURFACE AREA (AP) Fe_3O_4@SiO_2 *CORE SHELL*

Sample	Lus permukaan Ap (m2/g)				
	BET	Metode BJH		Metode DH	
		Adp	Desp	Adp	Desp
#1	204	53,14	80,36	53,52	81,35
#2	3,59	14,92	25,98	15,03	26,45
#3	3,39	6,67	12,11	6,77	12,37

Appear in Table 1, Table2 and Table 3, porous diameter (Dp), for each sample # 1, # 2 and # 3 experienced an increase (88.07; 912.8 and 205 Angstrom (A°)) BET method, but with BJH analysis method and decreased porous diameter DH:

Adsorption and Desorption (Table 1). The porous surface area decreased for the BET, BJH and DH methods, the largest prous surface area (Ap) in sample # 1: 204 m2 / g (BET), 53.14 m2 / g (BJH Adsorption), 80.36 m^2/g (Desorption-BJH); 53,52 m^2/g (Adsorption-DH) and 81,35 (Desorption-DH). And for vome porous (Vp) for BET method has increased (88.07 cm^3/g; 91.3 cm^3/g and 205 cm^3/g), according to BJH method and DH porous volume decreased, and the largest porous volume in sample #1: 754 cm^3/g (Adsorption-BJH); 17.20 cm^3/g (Desorption-BJH); 754 cm^3/g (Adsorption-DH) and 17.20 cm^3/g (Desorption-DH). Based on the BJH analysis and DH porosity (Dp, Ap and Vp) are consistent for each sample [17].

TABLE III. POROUS VOLUME (VP) Fe_3O_4@SiO_2 *CORE SHELL*

Sample	Porous volume (cm^3/g)				
	BET	BJH-Methode		DH-Methode	
		Adp	Desp	Adp	Desp
#1	88,07	754	17,20	754	17,20
#2	91,3	15,43	16,91	15,43	16,91
#3	205,7	17,04	15,23	17,04	15,23

D. Discussion

In Figure 8, the core-shell Fe_3O_4 @ SiO_2 morphology is contaminated with Pb (II) metal, after the adsorption process; there are some particles that are thought to come from contaminant material, Pb (II). This is supported by the results of the analysis with EDS, showing that there are detectable Pb atomic elements (0.24%) (see Figure 9). From the AAS test it is known that for sample # 1 has better absorption, this shows that Pb ions are not only pulled by magnetite Fe_3O_4 but also adsorbed by very porous SiO_2 [13], [18], [19].

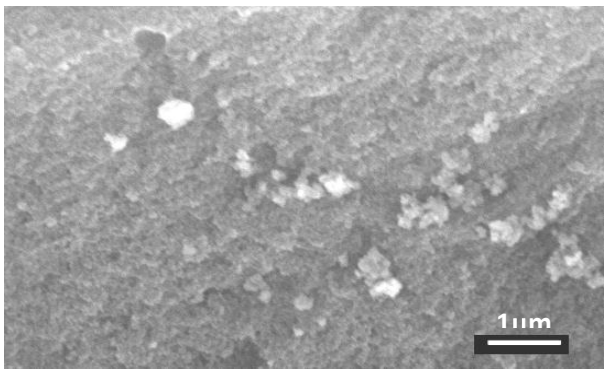

Fig. 8. SEM EDX nanocomposite $F_{e3}O_4$ @ SiO_2 test results which have been used as adsorbents.

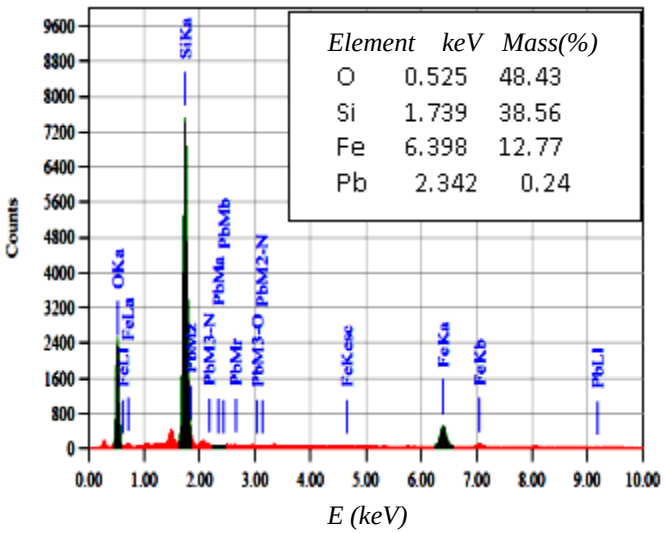

Fig. 9. EDX of Fe_3O_4 @ SiO_2 nanocomposite which has been used as an adsorbent.

Atomic Absorption Spectroscopy (AAS) is used to measure the concentration of atomic elements in solution. In this study, a solution containing PB (II) was sampled # 1, # 2 and # 3, to determine the absorption rate of Pb (II) by Fe_3O_4 @ SiO_2 Core-shell, with a duration of duration: 20 minutes; 40 minutes; 60 minutes; 80 minutes; and 100 minutes; where the initial state of the concentration of Pb (II) was 60 mg / l (pH 6), adsorption capacity, q_m was calculated, with Co initial concentration, C_e final concentration, V volume retained and M mass adsorbent [20].

$$q_m = \frac{C_o - C_e}{M} \times V \quad (1)$$

Seen during the initial immersion (20 minutes), the adsorption of Pb (II) metal has occurred very quickly, then in the next immersion period, there is a slow adsorption rate, and the overall time of soaking the amount of Pb (II) concentration absorbed more and more. Sample #1 shows the fastest adsorption capability: absorption capacity of 2.34 mg/g with absorbed Pb (II) concentration 23.4 mg /*l* [21]–[23].

IV. CONCLUSION

It has been successfully synthesized SiO_2, Fe_3O_4 and core-shell Fe_3O_4@ SiO_2/PEG nanoparticles, and microstructure and porosity analysis has been done by SEM-EDX and BET tests. The effect of the composition of Fe_3O_4 and SiO_2 on the Core-shell is that the more composition of SiO_2-NPs shows the porous properties and the larger particle size and vice versa. The most optimal application for adsorption on Pb (II) heavy metals is # sample-1 (1: 1).

ACKNOWLEDGMENT

Thank you to the Ministry of Research and Technology-Higher Education through the applied research of higher education institutions, which have provided funding support in research activities and this publication.

REFERENCES

[1] D. Chen et al., "Biocompatibility of magnetic Fe_3O_4 nanoparticles and their cytotoxic effect on MCF-7 cells," Int. J. Nanomedicine, p. 4973, Sep. 2012.

[2] J. Sun et al., "Synthesis and characterization of biocompatible Fe_3O_4 nanoparticles," J. Biomed. Mater. Res. A, vol. 80A, no. 2, pp. 333–341, Feb. 2007.

[3] C. Y. Haw et al., "Hydrothermal synthesis of magnetite nanoparticles as MRI contrast agents," Ceram. Int., vol. 36, no. 4, pp. 1417–1422, May 2010.

[4] L. Shen, B. Li, and Y. Qiao, "Fe_3O_4 Nanoparticles in Targeted Drug/Gene Delivery Systems," Materials, vol. 11, no. 2, p. 324, Feb. 2018.

[5] L. Bleney, Magnetite (Fe_3O_4): Properties, Synthesis, and Applications, vol. 15–2007. Lehigh University Lehigh Preserve: Lehigh University Lehigh Preserve, 2007.

[6] Y. F. Shen, J. Tang, Z. H. Nie, Y. D. Wang, Y. Ren, and L. Zuo, "Preparation and application of magnetic Fe_3O_4 nanoparticles for wastewater purification," Sep. Purif. Technol., vol. 68, no. 3, pp. 312–319, Aug. 2009.

[7] M. Munasir et al., "Composites of Fe_3O_4/SiO_2 from Natural Material Synthesized by Co-Precipitation Method," Mater. Sci. Eng., vol. 202, no. 2017, p. 12057, 2017.

[8] Munasir et al., "Composites of $Fe_3O_4@SiO_2$ from Natural Material Synthesized by Co-Precipitation Method," IOP Conf. Ser. Mater. Sci. Eng., vol. 202, p. 12057, May 2017.

[9] Munasir, N. R. D. Luvita, D. H. Kusumawati, N. P. Putri, Triwikantoro, and Z. A. I. Supardi, "Synthesis of PANi-SiO2 Nanocomposite with In-Situ Polymerization Method: Nanoparticle Silica (NPS) Amorphous and Crystalline Phase," J. Phys. Conf. Ser., vol. 997, p. 12052, Mar. 2018.

[10] S. Singh, K. C. Barick, and D. Bahadur, "Functional Oxide Nanomaterials and Nanocomposites for the Removal of Heavy Metals and Dyes," Nanomater. Nanotechnol., vol. 3, no. 20, 2013.

[11] Z. Luo, Y. Xu, and Q. Ye, "Effect of nano-SiO_2-LDPE packaging on biochemical, sensory, and microbiological quality of Pacific white shrimp Penaeus vannamei during chilled storage," Fish. Sci., vol. 81, no. 5, pp. 983–993, Sep. 2015.

[12] A. Priatama, M. Abdullah, K. Khairurrijal, and H. Mahfudz, "Fabrication of Microporous Water Filter Using Titanium Dioxide Particles, Silica Particles, and Polyethylene Glycol," ITB J. Eng. Sci., vol. 42, no. 1, pp. 39–52, 2010.

[13] I. Sheet, A. Kabbani, and H. Holail, "Removal of Heavy Metals Using Nanostructured Graphite Oxide, Silica Nanoparticles and Silica/ Graphite Oxide Composite," Energy Procedia, vol. 50, pp. 130–138, 2014.

[14] M. S. Beg, J. Mohapatra, L. Pradhan, D. Patkar, and D. Bahadur, "Porous Fe_3O_4-SiO_2 core-shell nanorods as high-performance MRI contrast agent and drug delivery vehicle," J. Magn. Magn. Mater., vol. 428, pp. 340–347, Apr. 2017.

[15] I. I. Lungu, M. RĂDULESCU2, G. D. MOGOŞANU, and A. M. GRUMEZESCU, "pH sensitive core-shell magnetic nanoparticles for targeted drug delivery in cancer therapy," Rom J Morphol Embryol, vol. 57, no. 1, pp. 23–32, 2016.

[16] A. Aghigh, V. Alizadeh, H. Y. Wong, M. S. Islam, N. Amin, and M. Zaman, "Recent advances in utilization of graphene for filtration and desalination of water: A review," Desalination, vol. 365, pp. 389–397, Jun. 2015.

[17] E. Karimi Pasandideh et al., "Silica-coated magnetite nanoparticles core-shell spheres ($Fe_3O_4@SiO_2$) for natural organic matter removal," J. Environ. Health Sci. Eng., vol. 14, no. 1, Dec. 2016.

[18] B. Saad Al-Farhan, "Removal of Cd^{+2} and Pb^{+2} Ions from Aqueous Solutions Using Bentonite-Modified Magnetic Nanoparticles," Int. J. Nanomater. Chem., vol. 2, no. 1, pp. 27–31, Jan. 2016.

[19] W. Cao, Y. Ma, W. Zhou, and L. Guo, "One-pot hydrothermal synthesis of rGO-Fe3O4 hybrid nanocomposite for removal of Pb(II) via magnetic separation," Chem. Res. Chin. Univ., vol. 31, no. 4, pp. 508–513, Aug. 2015.

[20] M. E. Chanani, H. Younesi, and N. Bahramifar, "Synthesis of Fe3O4@silica core– shellparticles and their application for removal of copper ions from water," Ournal Appl. Res. Water Wastewater, vol. 4, pp. 176–182, 2015.

[21] Y. Wei, B. Han, X. Hu, Y. Lin, X. Wang, and X. Deng, "Synthesis of Fe3O4 Nanoparticles and their Magnetic Properties," Procedia Eng., vol. 27, pp. 632–637, 2012.

[22] L. Wang, Z. Wang, H. Yang, and G. Yang, "The study of thermal stability of the SiO_2 powders with high specific surface area," Mater. Chem. Phys., vol. 57, no. 3, pp. 260–263, Jan. 1999.

[23] Q. Tian, X. Wang, F. Mao, and X. Guo, "Absorption performance of DMSA modified $Fe_3O_4@SiO_2$ core/shell magnetic nanocomposite for Pb2+ removal," J. Cent. South Univ., vol. 25, no. 4, pp. 709–718, Apr. 2018.